JACOBS PUBLISHERS

OPEN ACCESS

Jacobs Journal of Food and Nutrition

Review article

Eating Colors: A Scientifically based Perception of Food Colors

Ichiro Kasajima[1*], Rym Fekih[1]

[1]*Department of Agriculture, Iwate University, Ueda 3-18-8, Morioka, Japan*

**Corresponding author: Ichiro Kasajima, Department of Agriculture, Iwate University, Ueda 3-18-8, Morioka, Iwate 020-8550, Japan, Email: kasajima@iwate-u.ac.jp / kasajima2008@live.jp*

Received: 07-13-2016

Accepted: 12-13-2016

Published: 06-15-2017

Introduction

Humans, with our three cones-type visual systems, are probably better at distinguishing color than most mammals. Nevertheless, the common description of a particular color is considered to be 'subjective' since the surrounding environment has strong impacts on the color judgment. The basic way to estimate food color such as 'red' tomato, 'yellow' banana, 'green' parsley, and 'white' milk, terms that are also commonly used in academic papers in plant and food sciences, is qualified as a rough estimation of colors. Industries where color evaluation is one of the most important parts of the job, for instance, in the food industry, a scientifically based description is relevant for precise comparison of food colors. Therefore, we infer that analyzing the spectra of visible lights reflected by foods, with colorimetric functions is necessary. While the accurate measurement of colors is performed with a spectrophotometer, colors can also be measured with colorimeters and ordinary digital camera. All colors are defined with values of three factors, hue, lightness, and saturation [1]. After conversion of spectra of visible lights (380-780 nm) into RGB or XYZ colors with 'color matching functions', these three factors are calculated with various functions and plotted on diagrams. Representative diagrams include *round* diagram derived from RGB color and *L*a*b** diagram derived from XYZ color. In this report, we will show how to calculate colors, based on these diagrams.

Color matching functions

Colors are calculated from visible light spectra, based on color matching functions provided by the International Commission on Illumination (CIE, *Commission Internationale de l'Eclairage*, http://www.cie.co.at) [2]. There are two types of color matching functions, which are RGB color matching function and XYZ color matching function. For example, RGB color matching function is composed of three functions for red (R), green (G) and blue (B), respectively. Each function defines R, G and B values (intensities) every 5 nm starting from 380 nm to reach 780 nm. R, G and B values represent the amount of R, G and B colors included in the light at specific wavelengths. Therefore, color matching functions are more convenient if the original functions released from CIE is standardized so that the values throughout all visible wavelengths sum to unity [1]. Such standardized RGB color matching function is available in our previous report [3]. If naming this standardized RGB color matching function as F_R (for red), F_G (for green) and F_B (for blue), RGB intensities (I_R, I_G and I_B) are calculated from visible light spectra (*Spec*) at each wavelength (λ) as:

$$I_R = \Sigma_{(\lambda=380\text{-}780)}\, Spec(\lambda) \bullet F_R(\lambda)$$
$$I_G = \Sigma_{(\lambda=380\text{-}780)}\, Spec(\lambda) \bullet F_G(\lambda)$$
$$I_B = \Sigma_{(\lambda=380\text{-}780)}\, Spec(\lambda) \bullet F_B(\lambda)$$

Roughly speaking, light from 420 nm to 500 nm is blue, light from 500 nm to 580 nm is green, and light from 580 nm to 660 nm is red. This information is convenient for rough estimation of color from graphical data of light spectra. Cyanic lights around 500 nm have negative F_R values. RGB color matching function is based on colors of three existing lights (700 nm, 546.1 nm, and 435.8 nm), whereas XYZ color matching function uses imaginary colors to avoid using negative R values representing vivid cyanic colors. Y value of XYZ color matching function also corresponds to luminosity function, which calculates the way how human eyes sense brightness. Thus RGB color matching function goes in parallel to our sense of perceiving colors and would be suitable for intuitive understanding of food colors. XYZ color matching function, however, may be more systematically designed, and widely used for color calculations at the moment.

Measurement of light spectra

Next, how can we measure spectra of light which are reflected on the surface of foods, leaves, and flowers? Except for 'specular reflection' on mirrors, incident light is, once absorbed at the surface of a material, repeatedly reflected in the material, and goes out to random directions. This is known as 'diffuse reflection', which takes place on the surface of every food, leaf, and flower. During this process, specific wavelengths of lights are absorbed by pigments, then creating food colors. This process is just like white incident light entering a colored solution, which has color after coming out of the solution. Similar to the spectrophotometrical analysis of the absorbance of pigment solutions, reflection spectra of solid materials are measured with spectrophotometer equipped with a special attachment. UV/vis spectrophotometer UV-2450 (Shimadzu, Kyoto, Japan) is one of the machines available for measurement of surface reflectance.

All different light sources such as various fluorescent, incandescent and LED lights have different light spectra. Different spectra of incident light cause the different color of materials. Light spectra (spectral power distribution) of light sources can be measured with machines such as MS-720 Spectroradiometer (EKO Instruments, Tokyo, Japan). The spectrum of reflected light on food (*Spec*) is the multiplication between reflection spectrum (R) and incident light spectrum (L):

$$Spec(\lambda) = R(\lambda) \bullet L(\lambda)$$

Spectra of reflected lights are measurable, and RGB/XYZ colors of foods can be calculated following the aforementioned methods.

Plotting colors on diagrams

To understand colors of objects, RGB/XYZ color values have to be converted to hue, saturation and lightness values. Together with the calculation of these values, colors can be plotted on two-dimensional color diagrams through calculation of color coordinates. '*L*a*b** color coordinate' is derived from XYZ color values as follows [2]:

$$L^* = 116 \bullet Y^{1/3} - 16$$
$$a^* = 500 \bullet (X^{1/3} - Y^{1/3})$$
$$b^* = 200 \bullet (Y^{1/3} - Z^{1/3})$$

This is a simplified form of equations. The actual original equations are more complicated, but principally the same as these equations. In *L*a*b** color space, *L** represents lightness. Chroma (C^*_{ab}) and hue (h_{ab}) are calculated as follows:

$$C^*_{ab} = (a^{*2} + b^{*2})^{1/2}$$
$$h_{ab} = \arctan (b^*/a^*)$$

Here, 'chroma' is the absolute value of vividness. A similar term 'saturation' represents relative vividness. There is no upper limit for the value of chroma, whereas the maximum saturation value is unity [1]. *L*a*b** seems to be the most common color space adopted for comparison of plants colors. For example, colors of genetically modified rose and chrysanthemum were measured with *L*a*b** coordinates [4,5]. This would be partly because commercially available colorimeters automatically calculate *L*a*b** coordinates. In our opinion, a possible problem when plotting colors with *L*a*b** coordinates is that chroma value is distorted from linearity, by an inverse third-power function, when *a** and *b** values are calculated from XYZ color values. It seems to be generally thought that all colors are plotted in a color circle on *a*-b** diagram, but the actual area where all existing colors are plotted was not clear. Then we examined the shape of plotted area for saturated (100% vivid) colors on *a*-b** color plate. Here, *a** and *b** coordinates were calculated for saturated colors (every 5 nm from 380 nm to 780 nm), and purple colors (a serial mixture of extreme blue and extreme red), under the condition of 'X + Y + Z = 3' (Figure 1A). Red, yellow, green, cyan, blue and magenta are represented by plots of lights at 700 nm, 570 nm, 545 nm, 495 nm, 435 nm, and a 1:1 mixture of 780 nm and 380 nm. Contrary to expectations, the area of colors plotted on *a*-b** color plate greatly protruded a possible unit color circle (radius size of 100). The shape of the area was distorted, and hue angles of the above six colors were not evenly distributed. Hue angles of red, green and blue were approximately 45°, 135° and –45°. Colors plotted on *a*-b** color plate would fit better to a square as shown in the figure, rather than to a circle.

We recently reported calculation of '*round* diagram', which is derived from RGB colors [6]. In this diagram, color values are 'rounded' by three steps of calculations, to avoid distortion of the shape of plotted area. In our calculation system, lightness (L^{RGB}) is represented by the sum of I_R, I_G and I_B:

$$L^{RGB} = I_R + I_G + I_B$$

L^{RGB} is not based on luminosity function, but represents color intensity. 'Brightness' of the color could be independently calculated with luminosity function, if necessary. Next, relative ratios of red (ρ), green (ϒ) and blue (β) factors of the color is calculated:

$$\rho = I_R / L^{RGB}$$
$$\Upsilon = I_G / L^{RGB}$$
$$\beta = I_B / L^{RGB}$$

By using triangular vectors, colors are plotted on '*m-n* color plate':

$$(m, n) = (\rho - 1/2 \bullet \Upsilon - 1/2 \bullet \beta,\ \sqrt{3}/2 \bullet \Upsilon - \sqrt{3}/2 \bullet \beta)$$

Hue value (H^{RGB}) of this color is:

$$H^{RGB} = arctan2\ (\rho - 1/2 \bullet \Upsilon - 1/2 \bullet \beta,\ \sqrt{3}/2 \bullet \Upsilon - \sqrt{3}/2 \bullet \beta)$$

Saturation value (RGB) of this color is:

$$S^{RGB} = 1 - 3 \bullet min\ (\rho, \Upsilon, \beta)$$

Shape of plotted area on *m-n* color plate is distorted (Fig. 1B). Saturation values of cyanic colors (between green and blue) largely exceed 1 in this plot. Then saturation values of cyanic colors are approximated with ASSCC (approximated saturation of saturated cyanic colors):

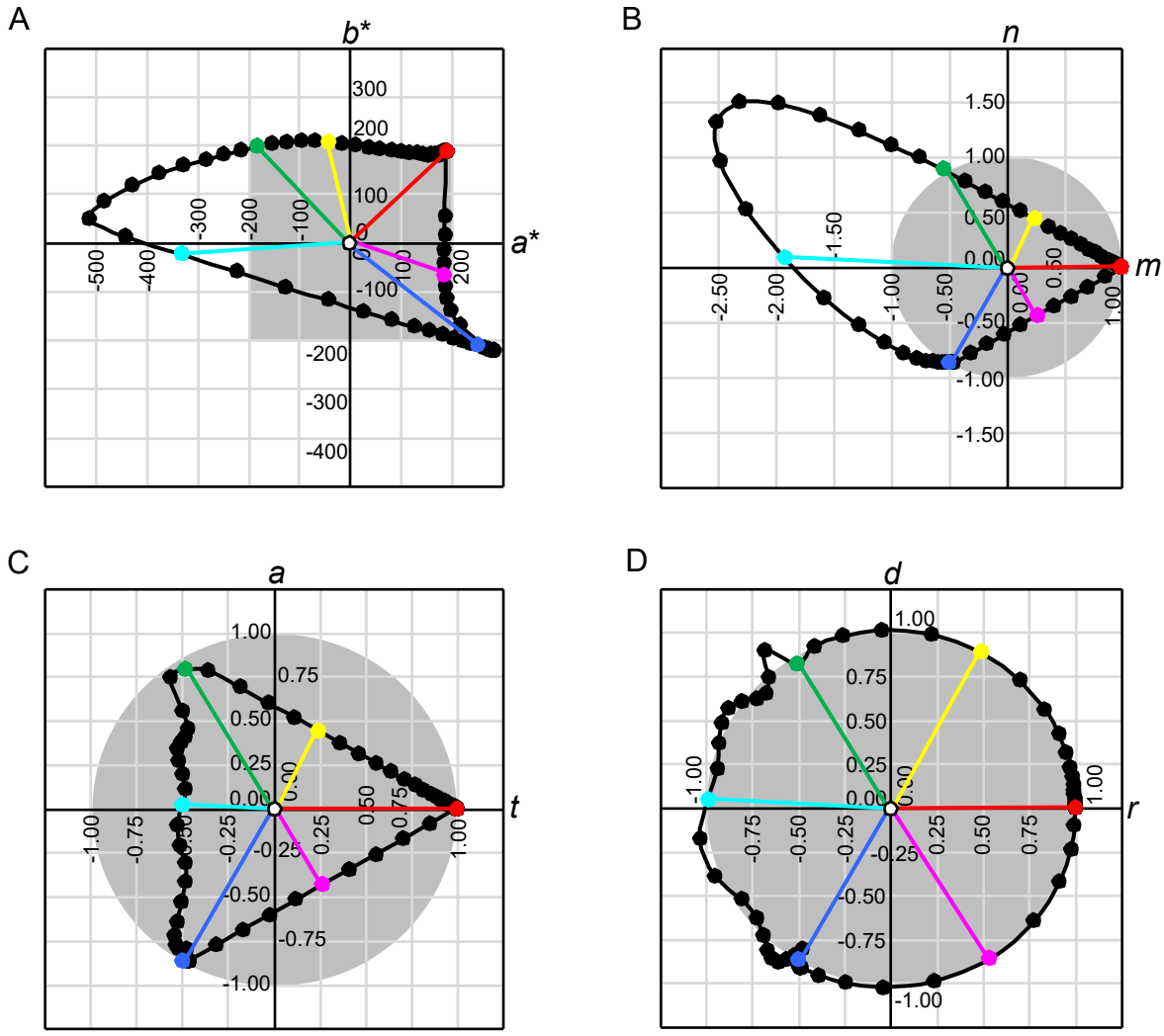

Figure 1. Areas of plotted visible colors in different diagrams.

Coordinates of saturated colors were calculated and plotted on (A) *a*-b** diagram, (B) *m-n* diagram, (C) triangle diagram, and (D) *round* diagram. Unit square for *a*-b** diagram and unit circles for *m-n*, *triangle*, and *round* diagrams are shown as gray areas. Approximate positions of saturated red, yellow, green, cyan, blue and magenta colors are shown with these colors, with lines connecting between the origin and these colors, for easy comparison of angles and distances from the origin.

$$ASSCC = 0.000\,000\,000\,203\,449\,043 \bullet (H^{RGB})^6 - 0.000\,000\,227\,268\,920 \bullet (H^{RGB})^5 + 0.000\,104\,570\,141 \bullet (H^{RGB})^4 - 0.025\,337\,245\,8 \bullet (H^{RGB})^3 + 3.405\,025\,71 \bullet (H^{RGB})^2 - 240.288\,362 \bullet H^{RGB} + 6\,950.267\,71$$

S^{RGB} value is corrected with ASSCC, to obtain a new saturation value (S^{RGB2}):

$$S^{RGB2} = S^{RGB} \quad (0° \le H^{RGB} \le 120°, 240° \le H^{RGB} \le 360°)$$
$$S^{RGB2} = S^{RGB} / ASSCC \quad (120° < H^{RGB} < 240°)$$

The corrected colors are plotted on '*triangle* color plate' with (t, a) coordinates (Fig. 1C):

$$(t, a) = (m, n) \quad (0° \le H^{RGB} \le 120°, 240° \le H^{RGB} \le 360°)$$

$$(t, a) = 1/ASSCC \bullet (m, n) \quad (120° < H^{RGB} < 240°)$$

Finally, colors are rounded with trigonometric functions, and plotted on *round* color plate with (r, d) coordinates (Fig. 1D):

$$r = S^{RGB2} \bullet \cos H^{RGB}$$
$$d = S^{RGB2} \bullet \sin H^{RGB}$$

Hue angles of the six representative colors are now evenly distributed around the color circle. Saturations values, expressed by the distance from the origin, is also nearly equal for any hue in the *round* diagram. Food colors will be better understood with this knowledge of actual color areas in these representative color diagrams.

Simple, convenient and rough measurement of food colors with digital camera

One might be interested to know about the difference between colorimeters and digital cameras, in term of measurement of colors. To understand the color-response features of digital cameras, we requested manufacturers of digital cameras to tell the response curves of RGB color filters, but they did not.

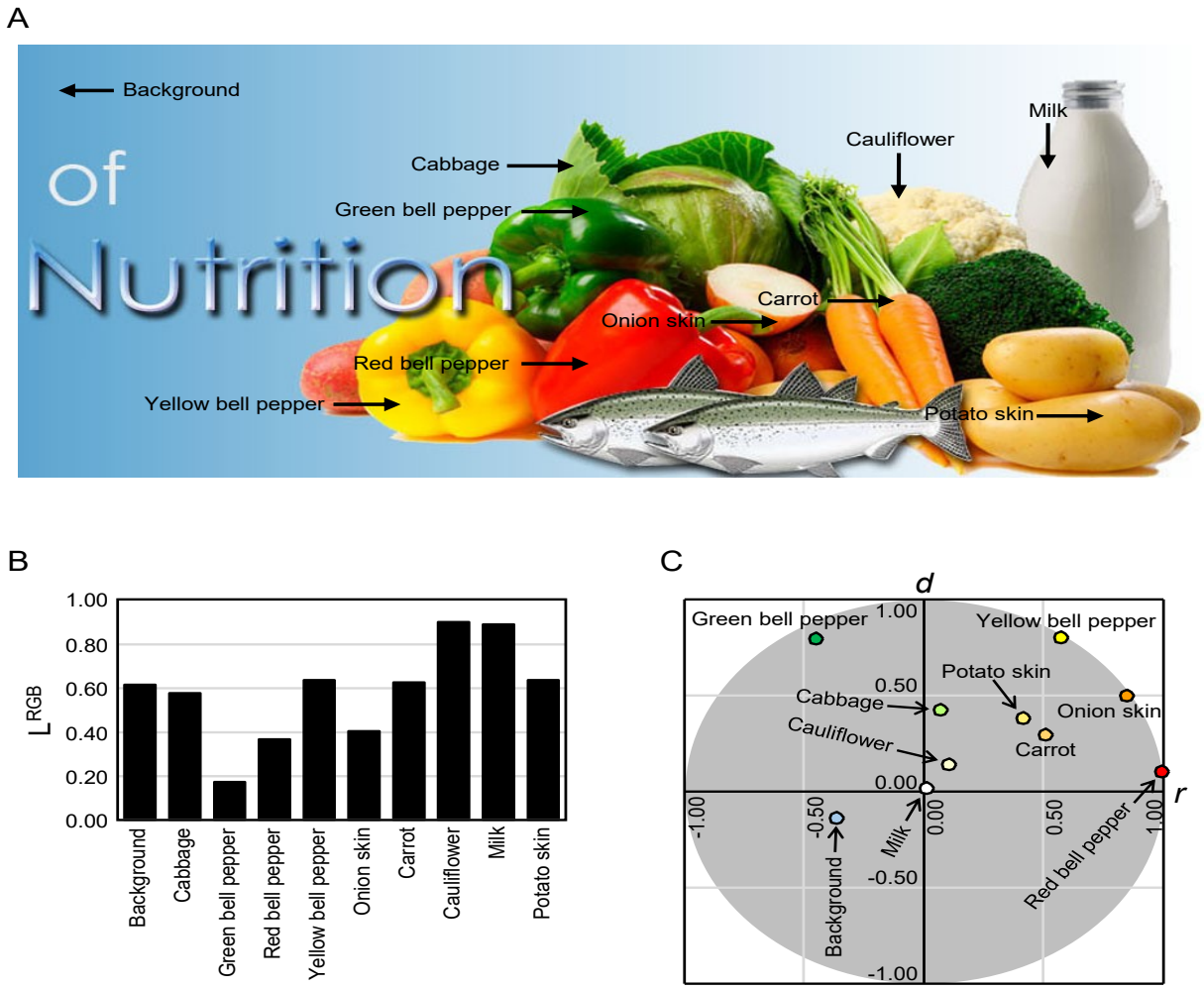

Figure 2. Calculation of food colors from digital photographs.

(A) Banner image used for calculation. Positions, where colors were sampled, are indicated with arrows. (B) The lightness of foods. (C) Food colors plotted on round diagram.

Thus we do not have access to precise information, but usually, it seems that response curves of RGB color filters equipped with digital cameras are quite different from RGB or XYZ color matching functions. Colors in pictures taken with digital cameras are similar to but different from actual colors.

Nevertheless, digital cameras are useful for rough estimation of food colors with relatively brief and easy processes.

In the rough estimation of digital photographs, RGB colors are sampled with Adobe Photoshop software, then parameters are calculated from these RGB values. As an example, colors of food pictures on the banner of this journal will be analyzed here. First, colors were sampled at ten different positions of the banner, as indicated in Figure 2A. These colors correspond to the background blue color, cabbage, green bell pepper, red bell pepper, yellow bell pepper, onion skin, carrot, cauliflower, milk and potato skin. Sampled RGB values and calculation of RGB parameters are shown in Table 1.

Food	R *	G *	B *	L^{RGB} **	ρ	γ	β	H^{RGB}	S^{RGB}
Background	91	168	209	0.61	0.19	0.36	0.45	200	0.42
Cabbage	158	198	84	0.58	0.36	0.45	0.19	80	0.43
Green bell pepper	5	124	4	0.17	0.04	0.93	0.03	120	0.91
Red bell pepper	252	27	0	0.36	0.90	0.10	0.00	6	1.00
Yellow bell pepper	255	227	3	0.63	0.53	0.47	0.01	54	0.98
Onion skin	202	103	2	0.40	0.66	0.34	0.01	30	0.98
Carrot	254	159	67	0.63	0.53	0.33	0.14	29	0.58
Cauliflower	254	245	190	0.90	0.37	0.36	0.28	53	0.17
Milk	231	228	223	0.89	0.34	0.33	0.33	38	0.02
Potato skin	232	182	71	0.63	0.48	0.38	0.15	42	0.56

* Saturated values of R, G and B are 255 here.

** Saturated value of L_{RGB} is 1 here.

Table 1. Calculation of food colors from the digital image.

Because R value of colors in digital photographs are always positive (or 0), unlike measurement of actual colors which can have negative R values, cyanic colors in digital photographs would be already folded within the RGB triangle. Then the calculation with ASSCC is omitted when estimating (*r, d*) coordinates for digital photographs. Lightness and plots on *round* diagram are also shown in Figure 2B and 2C. With this result, it is clarified that possibly against our sense of vegetable colors, onion skin is orange. Compared with carrot, hue angle of onion skin is nearly the same (approximately 30°), whereas onion skin is darker and more vivid than carrot. Cauliflower and yellow bell pepper are both yellow, but cauliflower is brighter and much less vivid than a yellow bell pepper. All bell peppers (red, yellow and green) are nearly 100% vivid, and we consumers may be attracted by their vivid colors when choosing to eat them, even if bell peppers are relatively expensive. Although being the same green vegetables, hue angles of green bell pepper and cabbage are quite different: Green bell pepper is green (H^{RGB} = 119°), but cabbage is yellow-green (H^{RGB} = 80°). This difference is related to mysterious colorimetric phenomena, which will be explained in the next chapter.

Colorimetric phenomena observed in foods and flowers

The color of foods and flowers are not necessarily stable. The color is sometimes affected by colorimetric phenomena, and change under different conditions [7-9]. First, a scientific explanation for such strange and mysterious phenomenon may have been the 'dichromatism' reported on the color of pumpkin seed oil [10,11]. The color of pumpkin seed oil is yellow-green at the edge of a spoon (where light path length is short), whereas the color of this oil is dark orange at the center of the spoon (where light path length is long). Previously, researches showed that pumpkin seed oil is colored by protochlorophyll pigment [12].

This finding may have been considered as a rare event, observed in food, where hue differs depending on pigment concentrations. But several years later, we also identified dichromatic effect in ordinary green leaves and popular red spices [3].

Figure 3A shows colors of green leaves. Looking at these leaves, it is clear that leaves of any plant are either dark green or light yellow-green: There are no light green or dark yellow-green leaves. This correlation between color and pigment (chlorophyll) concentration was clearly demonstrated by serial dilution of chlorophyll in an organic solvent (Fig. 3B). Again, leaf colors are principally determined by chlorophyll concentration. Leaves with a high concentration of chlorophyll are

dark green, and leaves with a low concentration of chlorophyll are light yellow-green. This principle agrees with colors of green bell pepper and cabbage measured in Figure 2. Painters empirically notice this law and commonly use dark green and light yellow-green color to paint leaves.

Figure 3C shows colors of red and orange spices (chili pepper, red bell pepper, turmeric, and saffron). Likewise, after serial dilution in an organic solvent, it was found that pigments contained in chili pepper and red bell pepper, or pigments contained in turmeric and saffron, have the same colors at the same concentrations.

On the other hand, red or orange pigments in these spices become yellow at low concentrations. To summarize, red pigments (probably carotenoids) are red at high concentration, orange at medium concentration, and yellow at low concentration, because of dichromatism. Considering this result, cooking yellow 'saffron rice' based on a red saffron (the dry pistils part of saffron flowers) ingredient, all make sense.

Another principle, related to flower colors was recently noticed: Colors of foods and flowers are certainly affected by spectra of lights under which they are illuminated. For example, sunlight, fluorescent light, incandescent light, and LED light all possess different light spectra.

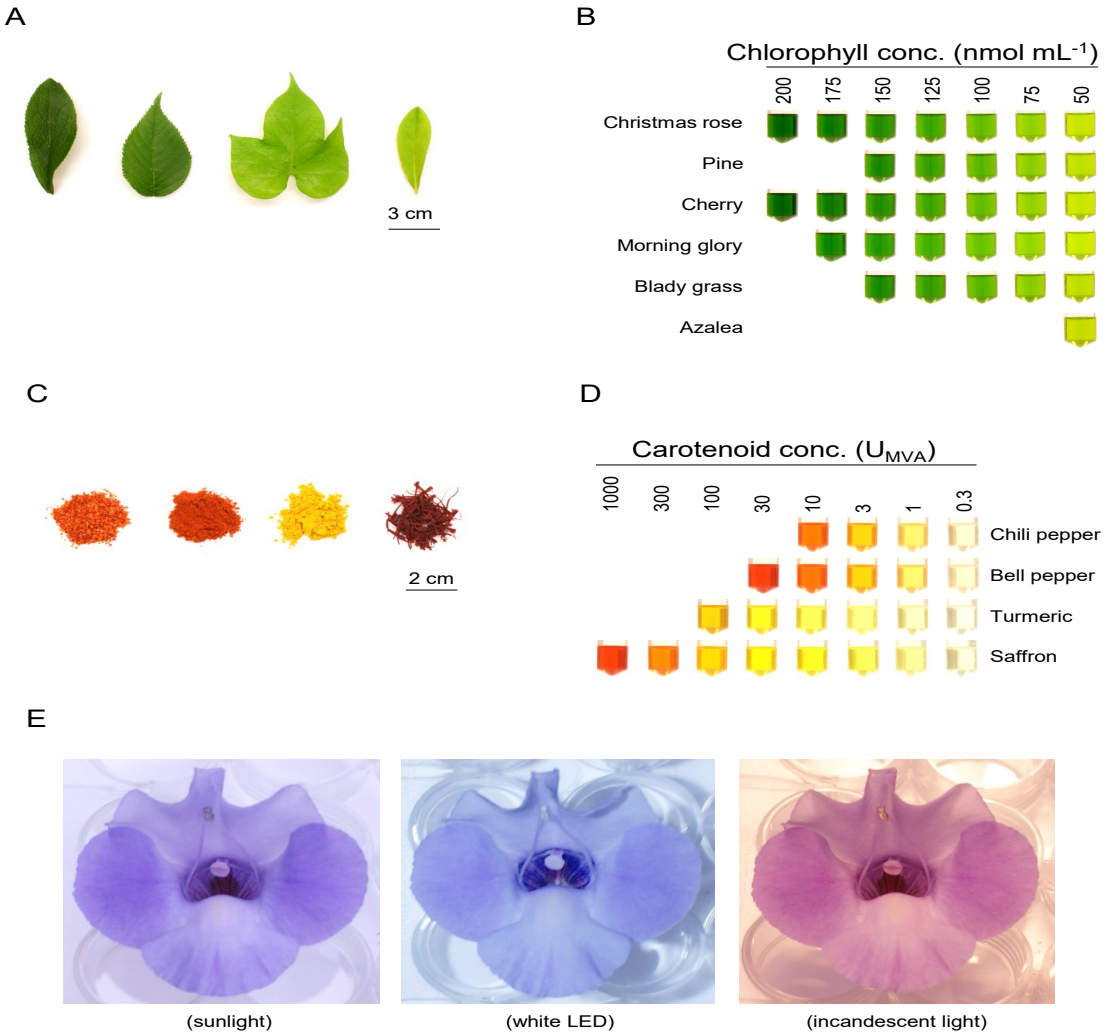

Figure 3. Dichromatism and alexandrite effect.

(A) Examples of plant leaves (Christmas rose, cherry, morning glory, and azalea). (B) Chlorophyll extracts from different plant species. Chlorophyll concentrations in organic solvent were adjusted as indicated in the figure. (C) Examples of red or orange spices (chili pepper, red bell pepper, turmeric, and saffron). (D) Carotenoid extracts from different spices. Carotenoid concentrations in organic solvent were adjusted as indicated in the figure. (E) Purple torenia flower (cultivar 'Summerwave Blue') observed under different incident lights (sunlight, white LED, and incandescent light). These photographs (from A through E) were taken from our previous reports [3,6].

Light spectra are also different between different kinds of fluorescent light or LED light, and between sunlight observed in different seasons, under different climates, and at a different time of a day. Thus, Foods have slightly different colors under different incident lights. Such susceptibility of the color is much more prominent in purple flowers (purple anthocyanin pigments). Purple flowers are purple under sunlight, but they are blue under white LED light or red under incandescent light. After spectrophotometric analysis, this effect was identified to be the same as that observed in gemstone alexandrite and was consequently called 'alexandrite effect' [13]. Figure 3E shows colors of 'purple' torenia flower, observed under sunlight, white LED, or incandescent light. Purple flowers specifically reflect blue and red lights. This is the reason why flowers easily become blue or red, according to the balance between blue reflection and red reflection. In the case of alexandrite, color is dependent on the balance between cyan reflection and red reflection.

Conclusion

Through utilization of a series of colorimetric functions, we became able to measure and precisely describe food and flower colors. Henceforth, it became even possible to predict food colors under different spectra of incident lights. Novel principles governing food colors, for instance 'dichromatism' and 'alexandrite effect', were recently clarified. These principles scientifically explain colorimetric phenomena which we discovered during our experiments. Now that we are probably able to better understand every aspect of food colors, we can cook and illuminate our dishes in a way that optimizes their tasty appearance, to further promote food industry and enjoy eating.

References

1. Hunt RWG, Pointer MR. Measuring Colour, 4th edition. Chichester, UK: Wiley, 2011.

2. CIE 015:2004. Colorimetry, 3rd edition. Vienna: Commission Internationale de l'Eclairage, 2004.

3. Kasajima I, Sasaki K. Dichromatism causes color variation in leaves and spices. Color Res Appl. 2015, 40: 605-611.

4. Katsumoto Y, Masako Fukuchi-Mizutani, Yuko Fukui, Filippa Brugliera, Timothy A. Holton et al. Engineering of the rose flavonoid biosynthetic pathway successfully generated blue-hued flowers accumulating delphinidin. Plant Cell Physiol. 2007, 48: 1589-1600.

5. Noda N, Aida R, Kishimoto S, Ishiguro K, Fukuchi-Mizutani M, Tanaka Y, Ohmiya A. Genetic engineering of novel bluer-colored chrysanthemums produced by the accumulation of delphinidin-based anthocyanins. Plant Cell Physiol. 2013, 54: 1684-1695.

6. Kasajima I. Alexandrite-like effect in purple flowers analyzed with newly devised round RGB diagram. Sci Rep. 2016, 6: 29630.

7. Eagerman BA, Clydesdale FM, Francis FJ. Comparison of color scales for dark colored beverages. J Food Sci. 1973, 38: 1051-1055.

8. Hutchings JB. Food Colour and Appearance. London, UK: Blackie Academic & Professional. 1994, 252-254.

9. Yang E, Kang H, Kim C, Pak CH. Dependence of the color appearance of some flowers on illumination. Color Res Appl. 2014, 39: 28-36.

10. Kreft S, Kreft M. Physicochemical and physiological basis of dichromatic color. Naturwissenschaften. 2007, 94: 935-939.

11. Kreft S, Kreft M. Quantification of dichromatism: A characteristic of color in transparent materials. J Opt Soc Am A. 2009, 26: 1576-1581.

12. Kreft M, Berden-Zrimec M, Zrimec A, Erdanikreft M, Kreft I, Kreft S. Pumpkin fruit, seed and oil yield is independent of fruit or seed photosynthesis. J Agric Sci. 2011, 149: 753-760.

13. White WB, Roy R, Crichton JM. The "alexandrite effect": and optical study. Am Mineral. 1967, 52: 867-871.